Manganese Schiff Base Immobilized on Graphene Oxide Complex and Its Catalysis for Epoxidation of Styrene

[1]Shuisheng Wu*, [1]Donghui Lan, [1]Nianyuan Tan, [2]Ran Wang, [1]Chak-Tong Au, [1]Bing Yi**
[1]Hunan Provincial Key Laboratory of Environmental Catalysis & Waste Recycling, School of Materials and Chemical Engineering, Hunan Institute of Engineering, Xiangtan 411104, China.
[2]School of Management, Hunan Institute of Engineering, Xiangtan, 411104, China.
wuss2005@126.com*; bingyi2004@126.com**

(Received on 12th September 2019, accepted in revised form 3rd December 2020)

Summary: Immobilization of metal complexes on solid supports is an efficient approach to circumvent the drawbacks of homogeneous catalysis. In this paper, using graphene oxide as carrier, manganese Schiff base supported on graphene oxide (Salen Mn-GO) was prepared through aminosilane covalent modification as well as salicylaldehyde condensation and coordination reaction. The structures and properties of the composite were examined by FT-IR, XRD, XPS, TEM, TG techniques, and the catalytic performance of Salen Mn-GO in styrene epoxidation was explored. The effects of catalyst and styrene amount as well as that of reaction time on the performance of the catalyst were investigated. The results showed that Salen Mn-GO has excellent catalytic activity and reusability for epoxidation of styrene in the presence of hydrogen peroxide. Finally, the mechanism of styrene epoxidation catalyzed by Salen Mn-GO has been preliminarily discussed.

Keywords: Graphene oxide; Schiff base; Manganese; Styrene; Epoxidation; Heterogeneous catalyst.

Introduction

Epoxides are widely used as intermediates for the production of fine chemicals, pharmaceuticals and perfumes, and much attention has been given to their generation [1-3]. The oxidizing agents commonly used in the preparation of epoxides are peraceticacid, t-butyl hydroperoxide (TBHP), sodium hypochlorite, high concentration hydrogen peroxide, etc. [4]. They are highly explosive and are applied in high concentration, leading to high safety requirements, product complication and poor selectivity to target product. These shortcomings restrict their industrial production, which is also a reason for the high prices of related pharmaceuticals and spices. In recent years, the use of hydrogen peroxide for olefin epoxidation has become a hot spot. With high effective oxygen content, it can be applied in concentration lower than that of strong oxidants such as oxyacetic acid and TBHP. It is ideal for epoxide synthesis because the requirements for equipment safety are not high. Furthermore, it is a green oxidant, and water is the only by-product [5-7]. To make the process economical and environmentally benign, it is necessary to design catalysts that can facilitate high selectivity to target product under green and safe conditions. It is a global desire to obtain stable catalysts of efficacy that can be facilely generated to catalyze the epoxidation of olefins using hydrogen peroxide as green oxidant.

In the search of oxidation processes that have application prospect, the use M-Salen complexes (M=Ti, Zr, Fe, Mn, Ni, Cu, Co, Zn, A1, etc) has come to the attention of researchers [8, 9]. Salen is a chelate Schiff base which can be used as ligand for the formation of metal complexes. It was reported that M-Salen exhibits good catalytic activity in photochemical synthesis [10], stereoselective epoxidation [11], cyclopropanation reaction [12], Diels-Alder addition [13], and polymerization [14]. As for the epoxidation of olefins, M-Salen complexes with simple structures were reported in recent years to show good catalytic activity, especially in catalytic asymmetric epoxidation. However, the M-Salen complexes were mainly applied in homogeneous reactions, and their application is somehow limited. Recently, the immobilization of Mn (III) salen complexes on insoluble solid carriers such as mesoporous materials, polymers, zeolites, clays, organic polymer inorganic hybrid materials has been extensively investigated [15-19]. As a new type of carbon material, graphene has received much attention in catalysis due to its good dispersibility, high specific surface area and stability in chemical environments. Moreover, it can be easily functionalized, and the surface of graphene oxide (GO) is usually rich with oxygen-containing groups (such as carboxyl, hydroxyl, and epoxy groups). With such functionalities, GO can be modified to a variety of composite materials. By anchoring organic or inorganic molecules onto its surface, GO properties can be diversified. The consequence is enlargement of application prospect of graphene-based materials in catalysis [20-25]. Su et al. reported transition metal Schiff base complexes immobilized on graphene as efficient and recyclable catalysts for epoxidation of styrene [26]. Zarnegaryan et al. prepared GO-supported copper(salen) complex for epoxidation of alkenes [27].

*To whom all correspondence should be addressed.

Allahresani et al. reported the covalent bonding of Ni (II) Schiff base complex onto GO sheets for the oxidation of alcohols [28].

In this paper, a functionalized graphene composite catalyst was prepared by using GO as support for the immobilization of Salen Mn catalyst by means of covalent bonding. The catalytic activity of the anchored catalyst was investigated in the epoxidation of olefins using a low concentration of hydrogen peroxide. The structure of the composite was analyzed by FT-IR, XRD, XPS, Raman and TG techniques. The reaction mechanism of the related reaction was discussed.

Experimental

Experimental reagent

Graphite, sulfuric acid, potassium permanganate, acetonitrile, 3-aminopropyltrimethoxysiloxane (APTMS), ethanol, salicylaldehyde, styrene, chlorobenzene, H2O2, and NaHCO3 of analytical grade were purchased from Shanghai Aladdin Chemical Reagent Co., Ltd., and were used without purification. Distilled water prepared in our laboratory was used in all the experiments.

Catalyst preparation

Synthesis of amino-functionalized graphene oxide (NH2-GO): Graphene oxide was prepared by a modified Hummers process [29]. The graphene oxide was ultrasonically dispersed in an ethanol solution to obtain a 0.5 mg mL-1 brownish yellow graphene oxide ethanol solution. Then 360 mL of the graphene oxide ethanol dispersion was placed in a three-necked flask. After the mixture was subject to 30 min of ultrasonication, an excess amount of 6.0 mmol APTMS in ethanol was added, and the reaction solution was refluxed for 6 h with stirring. After the reaction, the solid substance was filtered out and washed with a large amount of ethanol, and then dried under vacuum at 60°C for 3 h to obtain amino-functionalized graphene oxide (NH2-GO) which was brown in color.

Preparation of M-salen Complex anchored on GO: First 0.5 g of the prepared NH2-GO was dispersed in 30 mL of methanol, and excess salicylaldehyde (1.22 g, 10.0 mmol) was added to the suspension, and the resulted mixture was subject to reflux for 3 h. Afterward, the solid product was filtered out and washed with methanol three times to remove unreacted salicylaldehyde. After vacuum drying, the obtained powder was separately added with a certain amount of Mn(CH3COO)2·4H2O and an appropriate amount of methanol, and the mixture was stirred at room temperature for 12 h. The resulting solid substance was filtered out and washed with methanol several times to remove excess uncoordinated metal manganese ions, followed by vacuum drying at 60 °C for 2 h to obtain a graphene complex of "graphene oxide-loaded central metal Mn", which is herein named as Salen Mn-GO.

Characterization. Powder X-ray diffraction (XRD) analysis was performed on a Bruker D8 A25 diffractometer with a Cu Kα source (λ = 0.154 184 nm) at voltage of 40 kV and current of 40 mA. Infrared spectra were recorded on a Shimadzu IR Prestige-21 type Fourier transform infrared spectrophotometer with a wavenumber range of 400–4000 cm-1, adopting the KBr pellet approach. TEM images were obtained from a Tecnai G20 transmission electron microscope with a CCD imaging system at an acceleration voltage of 200 kV. Raman spectra were recorded by using excitation from the 514.5 nm line of an Ar-ion laser (Renishaw, RM 1000). XPS analysis was conducted on a PHI Quantera SXM with Al Kα = 1486.6 eV excitation source. Thermogravimetric analysis (TGA) was performed using a thermogravimetric analyzer (TG 209 F3 , Netzsch, Germany) under a flow of nitrogen.

Catalytic performance. Styrene epoxidation using CH3CN as solvent and H2O2 as oxidizing agent was carried out in a round bottom flask at 50 °C. First 100 mg of catalyst, 10 mmol of styrene, and 4 mL of CH3CN were added to a 25 mL single-neck round bottom glass vial. Then, a mixture of 1.36 g (12 mmol) of 30% H2O2 and NaHCO3 (0.2 mol/L, 4 mL) was added dropwise to the above solution under continuous stirring in a period of 0.5 h. After reacting at 50°C for 2 h, the reaction was terminated. The reaction solution after filtering off the catalyst through a membrane was analyzed by an Agilent 6890 N chromatograph equipped with Agilent DB-1 (30 m *0. 25 mm* 0. 25 μm) column and a flame ionization detector (FID). The chromatographic conditions were as follows: heating program 80°C for 2 min, 10°C /min to reach 200°C and then maintained for 5 min. As for injector and detector temperatures, they were 220°C. The solid catalyst was filtered off, washed thoroughly with acetone and dried at 60°C for 3 h for recycling without purification. Chlorobenzene was used as an internal standard to quantify components. Styrene conversion and styrene oxide selectivity are calculated according to the following formula:

$$\text{Styrene conversion} = \frac{\text{Amount of styrene before reaction - amount of residual styrene}}{\text{Amount of styrene before reaction}} * 100\%$$

$$\text{Styrene oxide selectivit y} = \frac{\text{Amount of styrene oxide produced}}{\text{Amount of styrene before reaction}} * 100\%$$

Results and Discussion

Material characterization

Fig 1 shows the X-ray diffraction patterns of graphite, GO, NH_2-GO, and Salen Mn-GO. As shown in Fig 1， graphite has a sharp diffraction peak at 26.5° (layer spacing d=0.335 nm) according to the Bragg equation $2d\ \sin(\theta)=\lambda$. Upon oxidation of graphite, the diffraction peak of GO at 10.8° (layer spacing d=0.79 nm) can be ascribed to the reflection of GO (001) plane, indicating that a large number of oxygen-containing groups have been introduced between the graphite layers, and the outcome is enlargement of interlayer spacing. After the loading of Salen complex, the characteristic peak of GO at 10.8° weakens but still exists, indicating that the modification does not destroy the sheet structure of graphene oxide. In the meantime, NH_2-GO and Salen Mn-GO show a wide and weak peak at 2θ=20–25°, which is the diffraction peak of amorphous silicon derived from 3-aminopropyltrimethoxysiloxane.

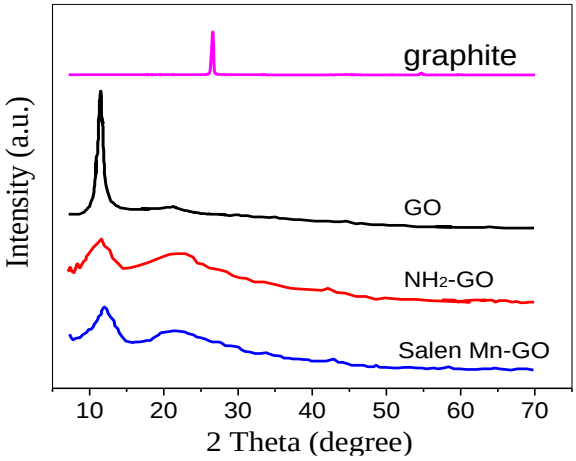

Fig. 1: XRD of graphite, GO, NH_2-GO and Salen Mn-GO.

Fig 2 shows the FT-IR spectra of GO, NH_2-GO and Salen Mn-GO. The broad band of GO spectrum at 3400 cm^{-1} is ascribable to hydroxyl groups. The absorption at 1724 cm^{-1} and 1626 cm^{-1} is correspond to the stretching vibration of C=O and C=C double bond, while that at 1050 cm^{-1} and 1217 cm^{-1} to C-O and C-OH single bond, respectively, which are consistent with the characteristic peaks of GO [30]. Compared to the FT-IR spectrum of GO, there are changes upon modification with silane coupling agent and salicylaldehyde. The NH_2-GO sample obtained after GO silanization exhibits significant signal enhancement at 1105 cm^{-1} and 1045 cm^{-1}, which is attributed to the absorption of Si-O-Si and Si-O-C bond, respectively. The tensile vibration peak of C-H bond at 2928 cm^{-1} confirms the presence of the aminosilicon chain. As for the Salen Mn-GO sample obtained after polycondensation with salicylaldehyde, it has the characteristic peaks of NH_2-GO, and there is sharpening of the peak at 1636 cm^{-1} that belongs to C=N. The new signals detected between 1400 cm^{-1} and 1600 cm^{-1} are due to the benzene ring of salicylaldehyde. These results confirm that there is successful anchoring of Mn Schiff base complex onto GO.

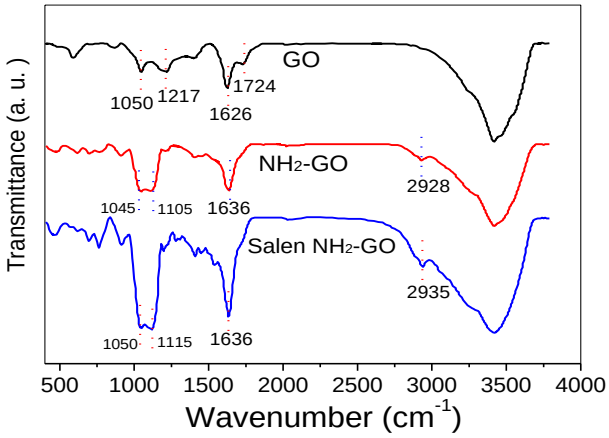

Fig. 2: FTIR spectra of GO, NH_2-GO and Salen Mn-GO.

Raman spectroscopy is often used to characterize the ordered and disordered structure of carbon materials (e.g., graphite, graphene, GO, etc.). Shown in Fig 3 are the Raman spectra of GO, NH_2-GO, and Mn-Salen-GO. The Raman plots of GO, NH_2-GO, and Mn-Salen-GO show two distinct bands at about 1334 cm^{-1} and 1596 cm^{-1}, commonly referred to as D and G bands, respectively. The G band is characteristic of carbon with sp^2 hybrid structure, which reflects the symmetry and crystallinity of graphene materials. As for the D band, it signifies the existence of defects in graphite [31]. The intensity ratio of D and G band, viz. ID/IG, is a unique parameter to indicate the graphitization level of graphite materials [31]. The ID/IG value of GO is ca. 1.1, while that of NH_2-GO and Mn-Salen-GO is ca. 1.19 and 1.21, respectively. The results indicate that the grafting of silane coupling agent and salicylaldehyde onto GO causes defects and/or deoxygenation [32]. It is observed that compared to the G band of GO at 1587 cm^{-1}, that of NH_2-GO and Mn-Salen-GO blue shifts to 1593 cm^{-1} and 1596 cm^{-1}, respectively, plausibly due to local stress caused by the increase of covalent bond chains.

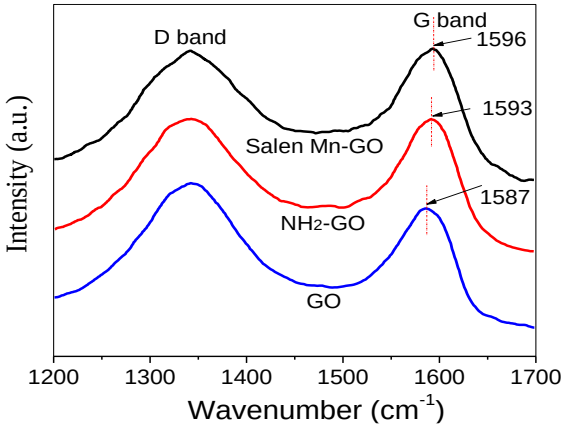

Fig. 3: Raman spectra of GO, NH_2-GO and Salen Mn-GO.

Fig. 4 shows the results of XPS analysis performed over GO, NH_2-GO and Salen Mn-GO. After silanization of GO, characteristic Si and N peaks can be observed in the NH_2-GO spectrum. Upon coordination with manganese acetate, Mn2p signals can be observed over the Salen Mn-GO sample. The results indicate successful immobilization of Salen Mn on GO. Fig 5(a) shows the deconvolution results of the C1s spectrum of GO, and the signals at ca. 284.8, 286.5, and 288.5 eV can be attributed to C-C, C=C, and C=O species, respectively. Fig 5(b) shows the C1s spectrum of NH_2-GO, and one can see decrease of C1s intensity at 286.5 eV, reflecting the involvement of hydroxyl groups during silanization of GO. Fig. 5(c) and Fig. 5(d) show the N1s spectra of NH_2-GO and Salen Mn-GO. After the condensation reaction of NH_2-GO with salicylaldehyde, most of the N-H bonds are converted to C=N bonds (399 eV). Furthermore, the binding energy of the C-N peak shifts from 399.6 to 399.9 eV, and that of NH_3^+ from 401.4 to 401.7 eV, which should be due to interaction between nitrogen atoms and Mn ions. In Fig. 6(a), the deconvolution of the Si 2p profile of NH_2-GO suggests two valence states corresponding to Si-O-Si and Si-O-C. The presence of Si-O-Si is due to self-polymerization of certain amount of silane coupling agent, and its presence cannot be eliminated by subsequent washing. The large presence of Si-O-C indicates the involvement of hydroxyl groups on GO is substantial during silylation. The Mn2p spectrum of Salen Mn-GO (Fig. 6(b)) shows Mn $2p_{3/2}$ and Mn $2p_{½}$ peaks at 641.8 eV and 653.5 eV, respectively, which are characteristic of divalent Mn [33]. Considering that the XPS technique is surface sensitive, the total manganese content was determined by inductively coupled plasma atomic emission spectrometry (ICP-AES), and was found to be 0.96 wt% (i.e., 0.17 mmol·g^{-1}).

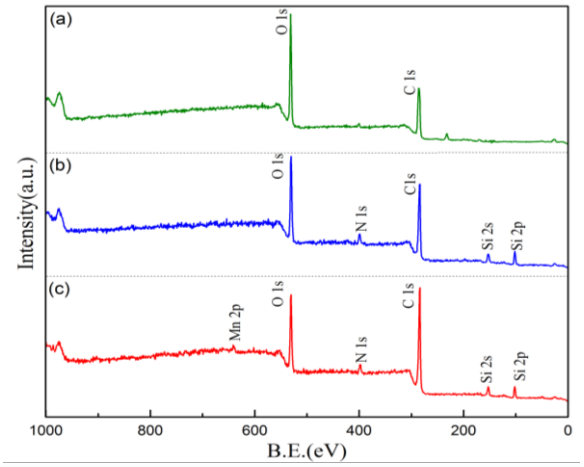

Fig. 4: Full range XPS spectra of (a) GO, (b) NH_2-GO(b) and (c) Salen Mn-GO.

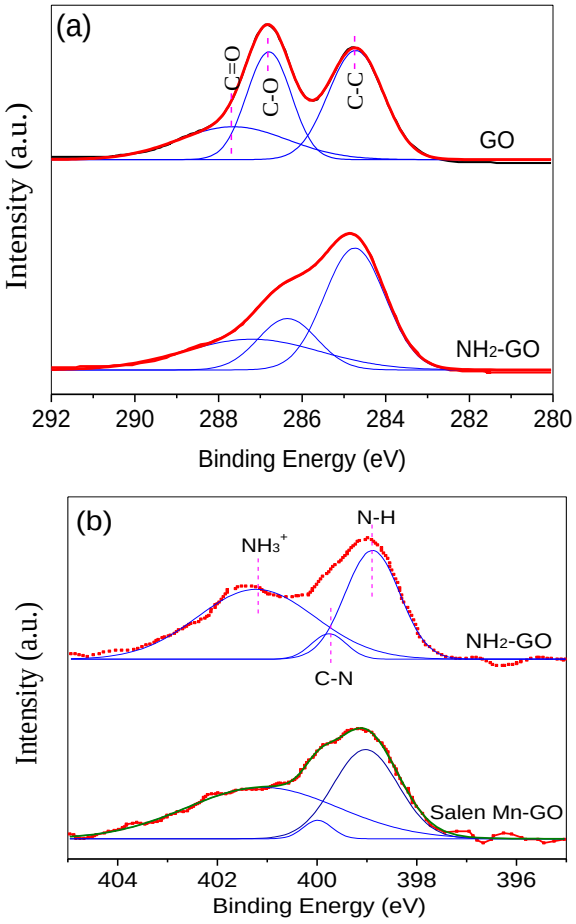

Fig. 5: (a) XPS C1s spectra of GO and NH_2-GO; (b) N1s spectra of NH_2-GO and Salen Mn-GO.

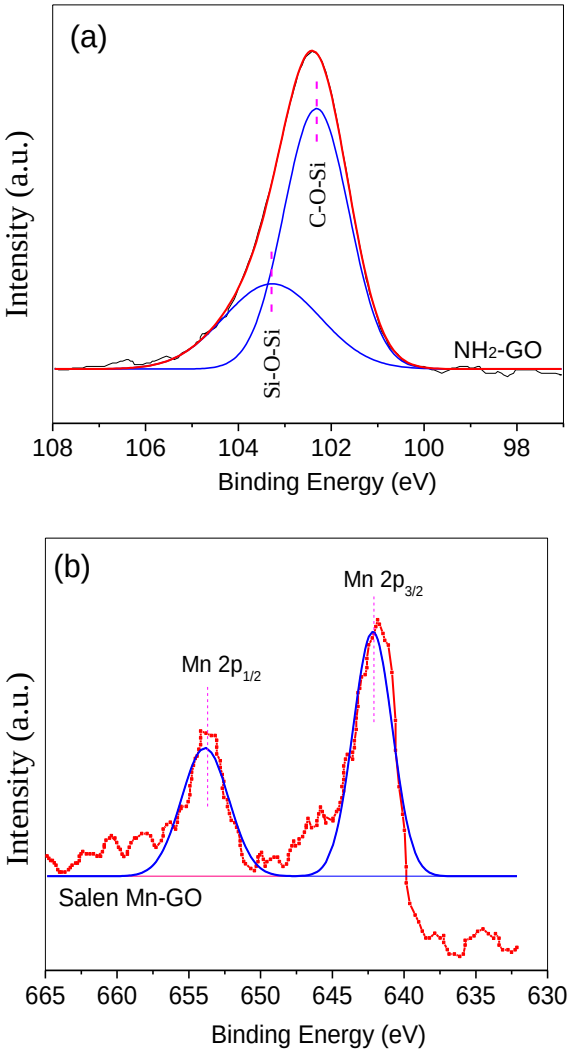

Fig. 6: (a) Si 2p spectrum of NH_2-GO and (b) Mn2p spectrum of Salen Mn-GO.

Fig 7 shows the thermogravimetric (TG) curves of GO and Salen Mn-GO. The TG curve of GO shows two significant weight losses in the range of 25–700 °C which belongs to the loss of physisorbed water and/or the decomposition of oxygen-containing functional groups [34]. Compared with GO, Salen Mn-GO shows a thermogravimetric curve that is relatively flat, and the mass loss in the interval of 100 to 150 °C is mainly caused by water loss; as for the mass loss at 150–300 °C, it is caused by the loss of undecomposed oxygen-containing groups. The mass loss above 300 °C is caused by the decomposition of metal Schiff base. According to the calculation based on Salen Mn-GO weight loss, the loading of Schiff base ligand Salen was about 0.35 mmol/g. As mentioned above, the Mn content based on ICP-AES analysis was 0.17 mmol/g. Hence, the ligand-to-metal molar ratio of Salem Mn-GO is close to 2:1. The above results indicate that the organometallic group has been successfully loaded onto GO.

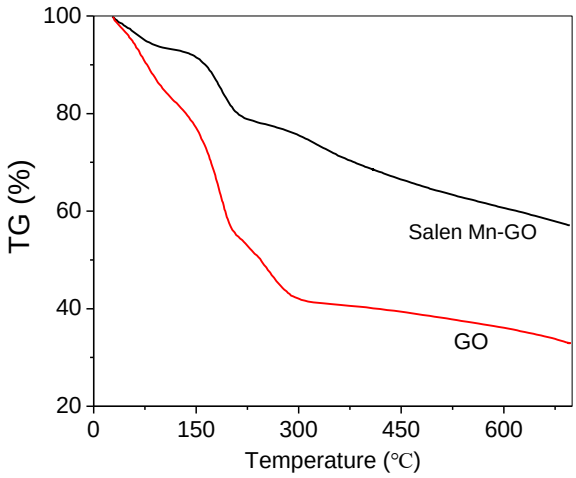

Fig. 7: TG curves of (a) GO and (b) Salen Mn-GO.

Transmission electron microscopy (TEM) images reveal the microstructure and morphology of the GO, NH_2-GO and Salen Mn-GO samples (Fig. 8a-c). Compared to the two-dimensional plane of GO, despite NH_2-GO and Salen Mn-GO still maintain a sheet-like structure, and they have more folds due to chemical modification. Without the destruction of the two-dimensional GO structure, the reaction sites of the supported catalyst are highly exposed to the reaction medium, and the GO surface serves as a platform for the entry of reactants and departure of products

Catalytic epoxidation of styrene

For comparison, we have also studied the catalytic performance of homogeneous complex catalysts. When acetonitrile was used as solvent and H_2O_2 as oxidant for styrene oxidation, the conversion of cyclooctene was 74.3% after 2 h of homogeneous reaction over the Mn-Salen catalyst, which is significantly lower than that of Mn-Salen-GO (99.5%). The results indicate that the catalytic active sites are Mn ions, and the Mn sites of the supported catalyst are isolated from one another.

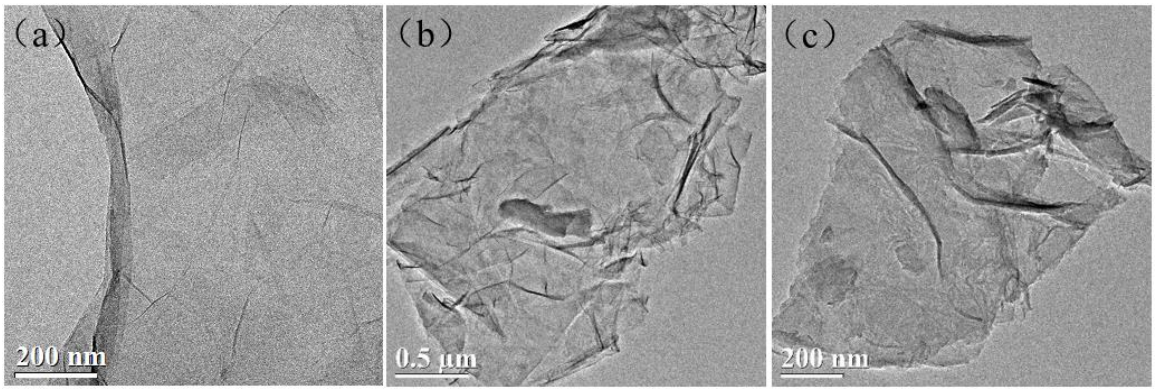

Fig. 8: TEM images of (a) GO; (b) NH_2-GO and (c) Salen Mn-GO.

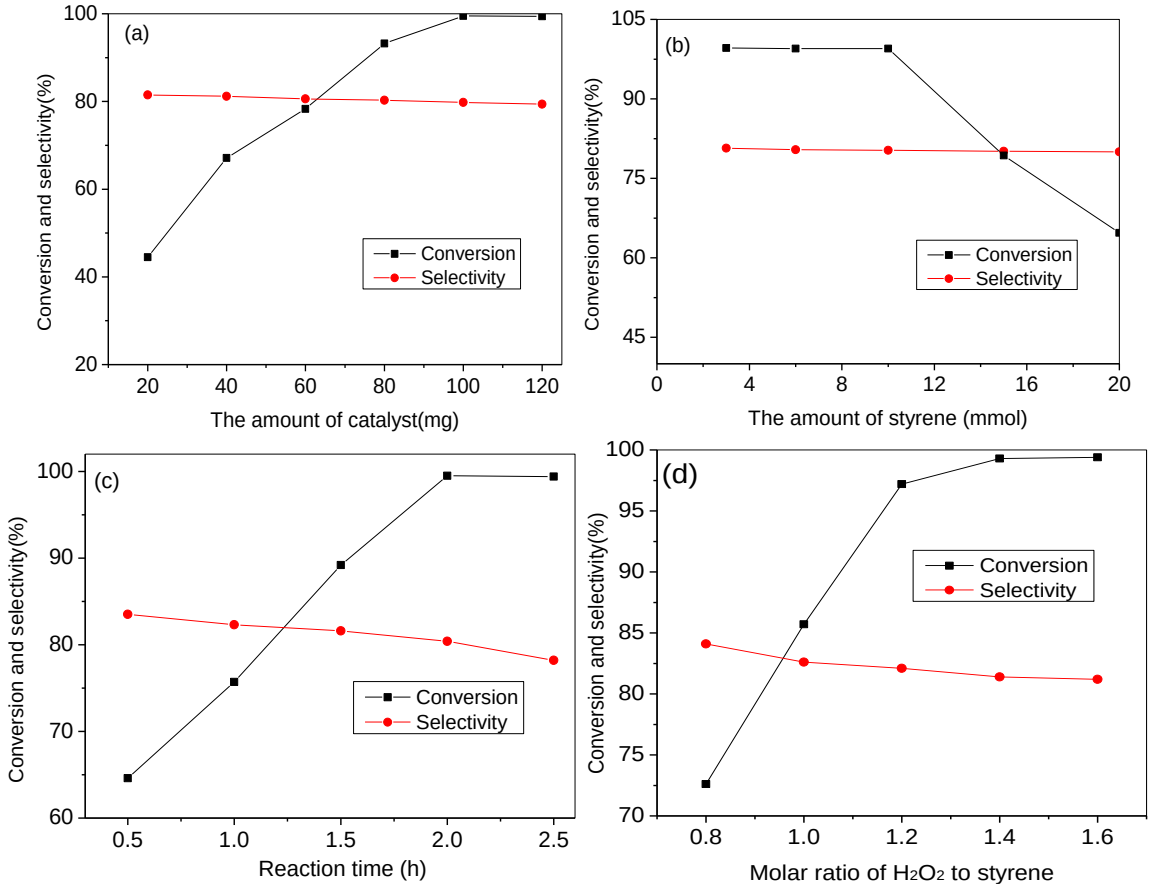

Fig. 9: Effect of (a) catalyst amount, (b) styrene amount, and (c) reaction time on styrene epoxidation over Salen Mn-GO, and (d) effect of H_2O_2-to-styrene molar ratio on the performance of Salen Mn-GO catalyst.

Fig 9 (a) shows the effect of the amount of Salen Mn-GO catalyst on styrene conversion and epoxy product selectivity. The amount of catalyst has a great influence on the conversion of styrene but has little effect on epoxide selectivity. With the other reaction parameters kept unchanged and the amount of catalyst increased from 20 to 120 mg, the conversion of styrene increased drastically from 44.5% to 99.5%, while epoxide selectivity decreased slightly from 81.5% to 79.4%. At a catalyst amount of 100 mg, the

conversion of styrene is the highest. Fig 9 (b) shows the effect of styrene amount on the epoxidation reaction. It was observed that the selectivity to epoxide is insensitive to the change of styrene amount, which stayed at about 80% with a change of styrene amount from 3 to 20 mmol. As for styrene conversion, it was ca. 99.5% during the change of styrene amount from 3 to 10 mmol. However, when the amount of styrene was increased from 15 to 20 mmol, styrene conversion decreased from 79.3% to 64.7%. Fig 9(c) illustrates the effect of reaction time on the epoxidation of styrene. When the reaction time increased from 0.5 to 2 h, the conversion of styrene increased from 64.6% to 99.5%, and there was slight decrease of epoxide selectivity from 83.5% to 80.4%. Further prolong of reaction had little effect on styrene conversion but resulted in slight decrease of selectivity. At reaction time of 2.5 h, styrene conversion was 99.4% and styrene oxide selectivity was 78.2%. When H_2O_2 is used as oxygen source, the H_2O_2-to-styrene molar ratio has a great influence on reaction activity. It can be seen from Fig 9(d) that the amount of H_2O_2 affects styrene conversion but has little effect on styrene oxide selectivity. When H_2O_2-to-styrene molar ratio increased from 0.8 to 1.4, the conversion of styrene gradually increased from 72.6% to 99.3% and remained unchanged with further increase of hydrogen peroxide. Therefore, the optimum H_2O_2-to-styrene molar ratio is 1.4.

In practical applications, the lifetime and reusability of the supported catalyst are important factors. We investigated the lifetime of the catalyst under the adopted reaction conditions. The specific method comprises the following steps: An appropriate amount of n-hexane was added to the system at the end of the reaction to extract reaction product. The reaction solution is statically layered, and the catalyst is dispersed in the aqueous phase. The organic phase and the aqueous phase were separated using a separation funnel. The aqueous phase was subject to filtration, washed with n-hexane and methanol, and dried in vacuo for repeat use. The results of activity change are shown in Fig. 10(a). Across five runs, styrene conversion and styrene oxide selectivity remain at a superior level, and there is no significant decrease of catalyst activity. Meanwhile, from the XRD patterns of fresh and recycled samples in Fig. 10 (b), there is no distinct difference in terms of crystal phase structure. The results show that the Salen Mn-GO catalyst has good stability in the epoxidation of styrene and could be reused for many times.

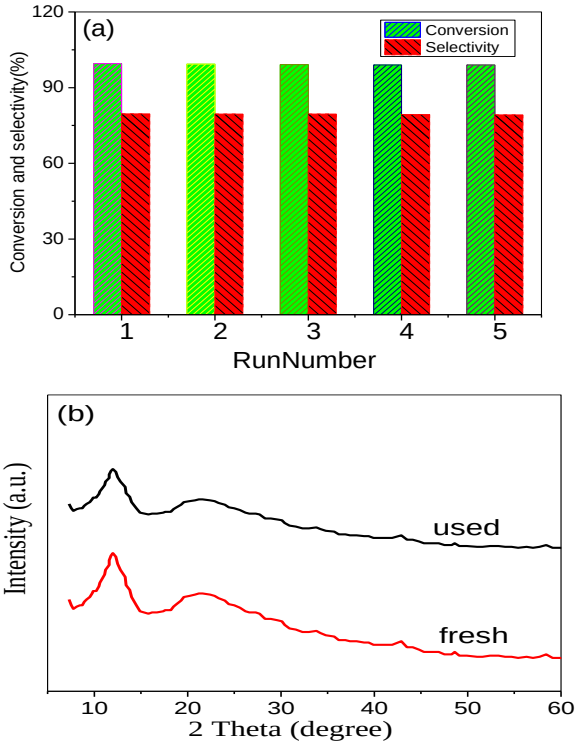

Fig. 10: (a)The reusability test of Salen Mn-GO catalyst.; (b) XRD patterns of Salen Mn-GO catalyst before and after use.

The heterogeneous properties of Salen Mn-GO catalyst were studied by hot filtration experiment. In the same reaction system, when the conversion of styrene was about 40%, the reaction solution was subject to filtration at 50 °C to remove the catalyst, and the filtrate allowed to react under the same reaction conditions. It was found that there was no further increase of styrene conversion in the filtrate after the thermal filtration. Also, no manganese was detected in the solution by ICP-AES, confirming no leaching of manganese into the solution. These results indicate that the Salen Mn-GO catalyst is stable during the reaction and the observed catalysis is heterogeneous in nature.

Table-1: Comparison of the efficiency of Salen Mn-GO with different heterogeneous Schiff base catalyst.

Entry	Catalyst	Time (h)	Oxidant	Conversion (%)	Selectivity (%)	References
1	Salen Mn-GO	2	H_2O_2	99.5	80.2	This study
2	Salen-GO	8	O_2	46.5	64.7	[38]
3	Cu(salen)-f-GO	12	TPHP	52.8	43.6	[39]
4	Salen Ni-GO	3	TPHP	91	99	[40]
5	PGO-salen-Co	6	H_2O_2	21	55.9	[41]
6	VO-salen-GO	8	O_2	89	74.5	[37]
7	Fe-salen-GO	8	O_2	77.5	90.2	[37]

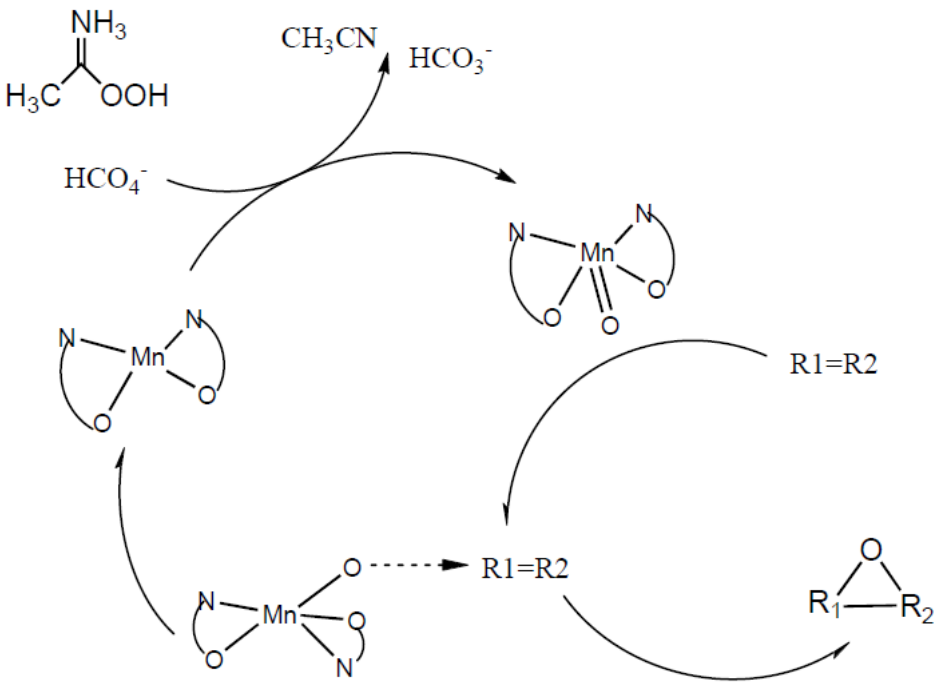

Scheme-1: Mechanism of styrene epoxidation catalyzed by Salen Mn-GO.

Despite the mechanism of olefin epoxidation by Schiff base complex is still uncertain, we conduct discussion on the catalytic epoxidation of olefins according to related literature [35-36]. In the reaction system, two kinds of catalyst assistants, viz. hydrogencarbonate and acetonitrile, react with hydrogen peroxide to produce two active intermediates:

$$HCO_3^- + H_2O_2 \rightleftharpoons HCO_4^- + H_2O$$

$$CH_3CN + H_2O_2 \rightleftharpoons$$

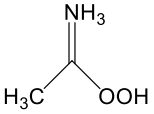

The two reactive intermediates are oxidizing agents which should interact with the olefinic substrate or first with the catalyst and then with the olefinic substrate. According to relevant literature [37] and referring to the reaction system, the following mechanism hypothesis is proposed as illustrated in Scheme-2: First, both bicarbonate and acetonitrile interact with H_2O_2 to form two oxidatively active intermediates. With themselves reduced, the two active intermediates oxidize Salen Mn-GO to form a reactive metal-oxide-containing peroxometal compound. Finally, the reactive oxygen-species-containing peroxometalate catalyst transfers the reactive oxygen atom to the alpha-pinene double bond. While the double bond is oxidized to an epoxy bond, the supported reactive intermediate is reduced and continues to react with the two reactive intermediates until the end of reaction. The specific mechanism is shown in Scheme-1. From the structure of Salen Mn, the benzene ring is conjugated with C=N to form an approximately planarπbond. The raw material styrene is affected by the π bond and tends to approach Salen Mn in a planar manner, thus producing mainly the epoxidized products.

Also, the results obtained using Salen Mn-GO in the epoxidation reaction was compared with the results reported for some other heterogeneous Schiff base catalysts. As can be seen, our reported method is superior in terms of reaction times, oxidant, yields or selectivity (Table-1).

Conclusion

In this paper, we prepared the heterogeneous catalyst Salen Mn-GO by means of stepwise grafting. The results of XRD, TEM, HR-TEM, FT-IR, Raman, XPS and TG characterization directly or indirectly confirmed the successful preparation of the target catalyst as well as the maintenance of the support structure during the grafting processes. The Salen Mn-GO catalyst was used in the epoxidation of styrene. It was observed that the supported catalyst has higher catalytic activity than the unsupported one, probably

due to the separation of the active centers in the former. In addition, the effects of catalyst and styrene amount as well as that of reaction time on the performance of the catalyst were investigated. In the reusability test, Salen Mn-GO did not significantly reduce in catalytic performance after repeated runs of styrene oxidation, indicating that the catalyst is stable and there is almost no loss of active sites during the reaction.

Acknowledgements

The project was supported by the National Natural Science Foundation of China (21772035), the Scientific Research Fund of Hunan Provincial Education Departmen (19B126), the Provincial Natural Science Foundation of Hunan(2018JJ3099), the Talent Research Startup Fund of Hunan Institute of Engineering (18RC009).

References

1 B. Angelique and M. E. Rehana, Olefin Epoxidation with Metal-Based Nanocatalysts, *Catal. Rev. Sci. Eng.*, **61**, 27 (2019).

2 X. Engelmann, D. D. Malik, T. Corona, K. Warm, E. R. Farquhar and M. Swart, Trapping of a Highly Reactive Oxoiron (IV) Complex in the Catalytic Epoxidation of Olefins by Hydrogen Peroxide, *Angew. Chem.-Int. Edit.*, **58**, 4012 (2019).

3 Q. He, Y. Zhang, H. Xiao, X. He, X. Zhou and H. Ji, Facile Synthesis of Metalloporphyrins-Ba^{2+} Composites as Recyclable and Efficient Catalysts for Olefins Epoxidation Reactions, *Chem. Res. Chin. Univ.*, **35**, 251 (2019).

4 R. V. Ottenbacher, E. Talsi and K. P. Bryliakov, Bioinspired Mn-aminopyridine Catalyzed Epoxidations of Olefins with various Oxidants: Enantioselectivity and Mechanism, *Catal. Today*, **278**, 30 (2016)

5 Q. Q. Chen, H. X. Zhang and J. X. Yang, $Pd(OAc)_2$-Catalyzed Synthesis of Benzyl Phenyl Ether Derivatives with H_2O_2 as an Oxidant in Neat Water, *Catal. Commun.*, **119**, 115 (2019).

6 H. Zou, G. Xiao, K. Chen and X. Peng, Noble Metal-Free V_2O_5/gC_3N_4 Composites for Selective Oxidation of Olefins Using Hydrogen Peroxide as an Oxidant, *Dalton Trans.*, *47*, 13565 (2018).

7 B. Qiu, D. Xu, Q. Sun, C. Miao, Y. M. Lee, X. X. Li and Sun, W, Highly Enantioselective Oxidation of Spirocyclic Hydrocarbons by Bioinspired Manganese Catalysts and Hydrogen Peroxide, *ACS Catal.*, **8**, 2479 (2018).

8 K. C. Gupta and A. K. Sutar, Catalytic Activities of Schiff Base Transition Metal Complexes, *Coord. Chem. Rev.*, **252**, 1420 (2008).

9 S. Yamada, Advancement in Stereochemical Aspects of Schiff Base Metal Complexes, *Coord. Chem. Rev.*, **190**, 537 (1999).

10 Ł. W. Ciszewski, K. Rybicka-Jasińska and D. Gryko, Recent Developments in Photochemical Reactions of Diazo Compounds, *Org. Biomol. Chem.*, **17**, 432 (2019).

11 A. Gualandi, C. M. Wilson and P. G. Cozzi, Stereoselective Reactions with Chiral Schiff Base Metal Complexes, *Chimia*, **71**, 562 (2017).

12 M. Bos, T. Poisson, X. Pannecoucke, A. B. Charette and P, Jubault. Recent Progress Toward the Synthesis of Trifluoromethyl-and Difluoromethyl- Substituted Cyclopropanes, *Chem.-Eur. J.*, **23**, 4950 (2017).

13 L. Li, Y. Li, D. Pang, F. Liu, A. Zheng, G. Zhang and Y. Sun, Highly Asymmetric Hetero-Diels–Alder Reaction Using Helical Silica-Supported Mn(III)-Salen Catalysts. *Tetrahedron*, **71**, 8096 (2015).

14 C. B. Durr and C. K. Williams, New Coordination Modes for Modified Schiff Base Ti(IV) Complexes and Their Control over Lactone Ring-Opening Polymerization Activity. *Inorg. Chem.*, **57**, 14240 (2018).

15 K. Yu, Z. Gu, R. Ji, L. L. Lou and S. X. Liul, Heterogeneous Chiral Mn(III) Salen Catalysts for the Epoxidation of Unfunctionalized Olefins Immobilized on Mesoporous Materials with different pore sizes, *Tetrahedron*, **65**, 305 (2009).

16 J. Zhang, L. Li, Y. Li, G. B. Zhang, A. Zheng, J. J. Zhang and Y. Sun, Immobilization of Chiral (salen) Manganese(III) Complexes Into Mesoporous Helical Silica for Asymmetric Epoxidation of Alkenes, *Catal. Lett.*, **145**, 1148 (2015)

17 V. Mirkhani, M. Moghadam, S. Tangestaninejad and B. Bahramian, A. Mallekpoor- Shalamzari, Host (nanocavity of zeolite-Y)-guest (manganese(III) salophen complex) nanocomposite materials: An Efficient Catalyst for Biomimetic Alkene Epoxidation and Alkane Hydroxylation with sodium Periodate, *Appl. Catal. A-Gen.*, **321**, 49(2007)

18 I. Kuzniarska-Biernacka, C. Pereira, A.P. Carvalho, J. Pires and C. Freire, Epoxidation of Olefins Catalyzed by Manganese(III) Salen Complexes Grafted to Porous Heterostructured Clays, *Appl. Clay Sci.*, **53**, 195 (2011)

19 M. A. Nasseri, A. Allahresani and H. Raissi, Grafting of a Chiral Mn(III) Complex on Graphene Oxide Nanosheets and its Catalytic Activity for Alkene Epoxidation, *Rsc Adv.*, **4**, 26087 (2014).

20 G. M. Scheuermann, L. Rumi, P. Steurer, W. Bannwarth and R.Mülhaupt, Palladium Nanoparticles on Graphite Oxide and its Functionalized Graphene Derivatives as Highly Active Catalysts for the Suzuki− Miyaura Coupling Reaction, *J. Am. Chem. Soc*., **131**, 8262 (2009).

21 X. Chen, G. Wu, J. Chen, X. Chen, Z. Xie and X. Wang, Synthesis of "Clean" and Well-Dispersive Pd Nanoparticles with Excellent Electrocatalytic Property on Graphene Oxide, *J. Am. Chem. Soc*., **133**, 3693 (2011).

22 Y. Yao, Z. Yang, H. Sun and S. Wang, Hydrothermal Synthesis of Co_3O_4–Graphene for Heterogeneous Activation of Peroxymonosulfate for Decomposition of Phenol. *Ind. Eng. Chem. Res.*, **51**, 14958 (2012).

23 Y. Liang, Y. Li, H. Wang, J. Zhou, J. Wang, T. Regier and H. Dai, Co_3O_4 Nanocrystals on Graphene as a Synergistic Catalyst for Oxygen Reduction reaction, *Nat. Mater*., **10**, 780 (2011).

24 Q. Zhao, C. Bai, W. Zhang, ,Y. Li, G. Zhang, F. Zhang and X. Fan, Catalytic Epoxidation of Olefins with Graphene Oxide Supported Copper (Salen) Complex, *Ind. Eng. Chem. Res.*, **53**, 4232 (2014).

25 S. Chaiyakun, N. Witit-Anun, N. Nuntawong, P. Chindaudom, S. Oaew, C. Kedkeaw and P. Limsuwan, Preparation and Characterization of Graphene Oxide Nanosheets, *Procedia Eng.*, **32**, 759 (2012).

26 H. Su, Z. Li, Q. Huo, J. Guan and Q. Kan,. Immobilization of Transition Metal (Fe^{2+}, Co^{2+}, Vo^{2+} or Cu^{2+}) Schiff Base Complexes onto Graphene Oxide as Efficient and Recyclable Catalysts for Epoxidation of Styrene. *RSC Adv.*, **4**, 9990 (2014).

27 A. Zarnegaryan, Z. Pahlevanneshan, M. Moghadam, S. Tangestaninejad, V. Mirkhani and I. Mohammdpoor-Baltork, Copper (II) Schiff Base Complex Immobilized on Graphene Nanosheets: a Heterogeneous Catalyst for Epoxidation of Olefins, *J. Iran Chem. Soc.*, **16**, 747 (2019).

28 A. Allahresani, Ni(II) Schiff Base Complex Immobilized on Graphene Oxide Nano-sheets Catalyzed Epoxidation of Alkenes, *J. Iran Chem. Soc.*, **14**, 1051 (2017).

29 B. J. Li , H. Q. Cao, J. Shao, G. Q. Li and G. Yin, Co_3O_4@graphene Composites as Anode Materials for High-Performance Lithium Ion Batteries, *Inorg. Chem.*, **50**, 1628 (2011).

30 G. Wang, X. Shen, J. Yao and J. Park, Graphene Nanosheets for Enhanced Lithium Storage In Lithium Ion Batteries, *Carbon*, **47**, 2049 (2009).

31 D. Pan, S. Wang, B. Zhao, M. Wu, H. Zhang, Y. Wang and Z. Jiao, Li Storage Properties of Disordered Graphene Nanosheets, *Chem. Mat.*, **21**, 3136 (2009).

32 W. Ai, J. Q. Liu, Z. Z. Du, X. X. Liu, J. Z. Shang, M. D. Yi and W. Huang, One-pot, Aqueous-Phase Synthesis of Graphene Oxide Functionalized with Heterocyclic Groups to Give Increased Solubility in Organic Solvents, *RSC Adv.*, **3**, 45 (2013).

33 W. Zheng, R. Tan, S. Yin, Y. Zhang, G. Zhao, Y. Chen and D. Yin, Ionic Liquid-Functionalized Graphene Oxide as an Efficient Support for the Chiral Salen Mn (iii) Complex in Asymmetric Epoxidation of Unfunctionalized Olefins, *Catal. Sci. Technol.*, **5**, 2092 (2015).

34 H. P. Mungse, S. Verma, N. Kumar, B. Sain and O. P. Khatri, Grafting of Oxo-Vanadium Schiff Base on Graphene Nanosheets and its Catalytic Activity for the Oxidation Of Alcohols, *J. Mater. Chem.*, **22**, 5427 (2012).

35 B. S. Lane and K. Burgess, A Cheap, Catalytic, Scalable, and Environmentally Benign Method for Alkene Epoxidations, *J. Am. Chem. Soc*., **123**, 2933(2001).

36 B. S. Lane, M. Vogt, V. J. DeRose and K. Burgess, Manganese-catalyzed Epoxidations of Alkenes in Bicarbonate Solutions, *J. Am. Chem. Soc*., **124**, 11946 (2002).

37 Z. Li, S. Wu, H .Ding, H. Lu, J. Liu, Q. Huo and Q. Kan, Oxovanadium (IV) and Iron (III) Salen Complexes Immobilized on Amino-Functionalized Graphene Oxide for the Aerobic Epoxidation of Styrene, *New J. Chem.*, **37**, 4220 (2013).

38 Z. Li, S. Wu, H. Ding, D. Zheng, J. Hu, X. Wang, Q. Huo, J. Guan and Q. Kan, Immobilized Cu(II) and Co(II) Salen Complexes on Graphene Oxide and their Catalytic Activity for Aerobic Epoxidation of Styrene, *New J. Chem.*, **37**, 1561 (2013).

39 Zhao, C. Bai, W. Zhang, Y. Li, G. Zhang, F. Zhang and X. Fan, Catalytic Epoxidation of Olefins with Graphene Oxide Supported Copper (Salen) Complex, *Ind. Eng. Chem. Res.*, **53**, 4232 (2014)

40 M. Nandi, P. Roy, H. Uyama, and A. Bhaumik, Functionalized Mesoporous Silica Supported Copper(II) and Nickel(II) Catalysts for Liquid Phase Oxidation of Olefins, *Dalton Trans*., **40**, 12510 (2011)

41 J. Sun, J. Zhang, L. Wang, L. Zhu, X. Meng and F. Xiao, Co-Salen Functionalized on Graphene as An Efficient Heterogeneous Catalyst for Cyclohexene Oxidation, *J. Energy Chem.*, **22**, 48 (2013).